Raman and optical absorption spectroscopic investigation of Yb-Er codoped phosphate glasses containing SiO_2

Youkuo Chen (陈尤阔)[1*], Lei Wen (温 磊)[1], Lili Hu (胡丽丽)[1], Wei Chen (陈 伟)[1], Y. Guyot[2], and G. Boulon[2]

[1]*Shanghai Institute of Optics and Fine Mechanics, Chinese Academy of Sciences, Shanghai 201800*

[2]*Physical Chemistry of Luminescent Materials, University of Lyon, UMR CNRS 5620, Villeurbanne 69622, France*

[*]*E-mail: chenyoukuo@yahoo.com*

Received April 30, 2008

Yb-Er codoped Na_2O-Al_2O_3-P_2O_5-$x SiO_2$ glasses containing $0-20$ mol% SiO_2 were prepared successfully. The addition of SiO_2 to the phosphate glass not only lengthens the bond between P^{5+} and non-bridging oxygen but also reduces the number of P=O bond. In contrast with silicate glass in which there is only four-fold coordinated Si^{4+}, most probably there coexist $[SiO_4]$ tetrahedron and $[SiO_6]$ octahedron in our glasses. Within the range of $0-20$ mol% SiO_2 addition, the stimulated emission cross-section of Er^{3+} ion only decreases no more than 10%. The Judd-Ofelt intensity parameters of Er^{3+}, Ω_2 does not change greatly, but Ω_4 and Ω_6 decrease obviously with increasing SiO_2 addition, because the bond between Er^{3+} and O^{2-} is more strongly covalently bonded.

OCIS codes: 160.2750, 160.5690, 300.6450, 300.6170.

doi: 10.3788/COL20090701.0056.

Yb-Er codoped phosphate laser glasses are widely used in optical communication, eye-safe range-finding, and lidar application[1]. However, the low thermal damage threshold of present phosphate hosts severely limits the output power/energy and repetition rate of Yb-Er glass lasers. At present, one of the important issues in the development of Er-doped laser glass is how to improve the thermal shock resistance without deteriorating the spectroscopic and laser performance greatly.

Surface processing, such as ion exchange process, has been applied to strengthen Er-doped phosphate glasses successfully[2]. Regarding the glass host, Al_2O_3 is usually used as a component to modify the glass structure and increase the thermal-mechanical properties of phosphate glasses[3,4]. Kigre's QX/Er glass[5] contains up to 14 mol% Al_2O_3, and the thermal loading capability of this glass was proved to be two times larger than that of another commercial Er-doped phosphate glass[5]. However, the main problem of Al_2O_3 addition is that the emission cross-section of Er^{3+} is reduced with increasing Al_2O_3 content. It was reported[6] that the emission cross-section of Er^{3+} in phosphate glass decreases from 0.74×10^{-20} to 0.56×10^{-20} cm^2 as the Al_2O_3 content increases from 4% to 13%.

Silicate based glass is mechanically stronger and chemically more stable than phosphate based glass. Attempts have been made to strengthen phosphate laser glasses by introducing SiO_2. A lithium phosphate glass containing up to 30 mol% SiO_2 was developed as a Nd-doped laser glass[7]. Such a silicophosphate glass exhibits a lower thermal expansion coefficient of $70\times10^{-7}-80\times10^{-7}/°C$, compared with the values of $120\times10^{-7}-130\times10^{-7}/°C$[8] for most of commercial Nd-doped phosphate glasses.

In this letter, some amount of SiO_2 was introduced into the Yb-Er co-doped Na_2O-Al_2O_3-P_2O_5 glass system. By Raman analysis, the structural evolution induced by the addition of SiO_2 was investigated. With the optical absorption spectroscopic analysis, the relationship between the glass structure-composition and the spectroscopic parameters was discussed.

Phosphate based glasses with the composition of $(79.5-x)(0.94P_2O_5$-$0.06Al_2O_3)$-$15Na_2O$-$xSiO_2$-$5Yb_2O_3$-$0.5Er_2O_3$ ($x = 0$, 5, 10, 15, and 20 mol%) were prepared successfully by traditional melting method. Analytical grade powders of P_2O_5, $Al(H_2PO_4)_3$, NaH_2PO_4, SiO_2, and 99.99% high purity powders of Yb_2O_3 and Er_2O_3 were used as raw materials. About 100-g well-mixed powders were melted in covered silica crucible for 60 min in the temperature range from 1300 to 1450 °C, depending upon glass composition. The melt was moulded into a cuboid piece on a preheated steel plate and then transported to a preheated muffle furnace. Glass samples were annealed for 120 min at a temperature from 440 to 460 °C, depending on glass composition, and cooled to room temperature at a rate of 20 °C per hour. All glass samples are clear and bubbles free. Samples with the size of $20\times10\times2$ (mm) were cut out and polished for spectroscopic measurements.

The Raman spectra were measured using Jobin Yvon LabRam-1B Confocal Raman Microscope excited by a He-Ne laser. The fact that Raman spectra detected at different part of a sample have almost the same Raman bands for band position and intensity indicates that the glass sample is homogeneous in composition and structure. Perkin-Elmer Lambda 900 UV/VIS/NIR double-beam spectrophotometer was used to obtain the absorption spectra in the wavelength range from 300 to 1700 nm. In the wavelength region without absorption of rare earth ions, the fact that there is almost no absorption intensity indicates that the glasses have highly optical quality. By exciting the glass samples with a 974-nm, 0.5-W InGaAs laser diode, the emission spectra of Er^{3+} were detected using Jobin Yvon TRIAX 550 spectrometer. All measurements were conducted at room temperature.

Phosphate glass mainly consists of $[PO_4]$ tetrahedrons,

which are linked by bridging oxygen ions to form phosphate chains. The symbol Q^n is used to represent a $[PO_4]$ tetrahedron, where n is the number of bridging oxygen ions in a given tetrahedron. For example, a Q^3 unit has three bridging oxygens and one terminal oxygen with P=O double bond, while a Q^2 unit has two bridging oxygens and two non-bridging oxygens.

Figure 1 shows the Raman spectra of the phosphate glass samples with different SiO_2 content in the region of $500 - 1450$ cm^{-1}. The spectra were normalized to the band at 1200 cm^{-1} and the outline of the Raman spectra almost remains unchanged with the addition of SiO_2. But it is obvious from Fig. 1 that the position and relative intensity of Raman bands are really affected by the introduction of SiO_2. No extra band related to Si–O bond has ever emerged in the spectra even though the addition of SiO_2 is up to 20 mol%. But it must be remembered that Si–O produces weak bands at around 600 and 1100 cm^{-1} that are easily hidden by the relatively higher intensity of P–O bands[9].

The Raman spectra of Na_2O-P_2O_5[10,11] and Na_2O-Al_2O_3-P_2O_5[12] glasses have been extensively studied and peak assignments have been made. As our glass samples have similar compositions with those reported in literatures, an assignment is indicated as shown in Fig. 1. The band at about 700 cm^{-1} is attributed to $(POP)_{sym}$ mode, the symmetric stretching of bridging oxygen ions that link neighboring tetrahedrons. With increasing content of SiO_2, the relative intensity of this $(POP)_{sym}$ mode decreases unremarkably and its peak position remains nearly unchanged. The bands locating at near 1210 and 1260 cm^{-1} are respectively assigned to $(PO_2)_{sym}$ and $(PO_2)_{asym}$ mode, the symmetric and asymmetric stretching of non-bridging oxygens in Q^2 tetrahedrons. Figure 1 demonstrates that the $(PO_2)_{sym}$ peak moves from 1210 cm^{-1} (0 mol% SiO_2) to 1175 cm^{-1} (20 mol% SiO_2). It is noteworthy that as the SiO_2 content increases in the glass, the $(PO_2)_{sym}$ mode shifts to lower frequency while the $(POP)_{sym}$ mode is almost fixed at 700 cm^{-1}, although these two peaks are both stretching mode due to Q^2 units. The behavior of $(POP)_{sym}$ mode indicates that the bridging oxygen is hardly affected by the introduction of SiO_2. The reduction in frequency of $(PO_2)_{sym}$ mode is related to an increase for average bond length between P^{5+} and non-bridging oxygen. Accordingly, Si^{4+} ions in our glass system probably tend to bond to those non-bridging oxygen in Q^2 units.

In Fig. 1, the wide band at $1300 - 1350$ cm^{-1} is attributed to the P=O stretching mode in Q^3 units. The sample with 5 mol% SiO_2 has a much weaker Raman band of P=O stretching mode than the sample without SiO_2 addition. The decrease for the intensity of P=O mode is related to the reduction for the amount of P=O bond. But with further addition of SiO_2, the intensity of P=O mode decreases much slower.

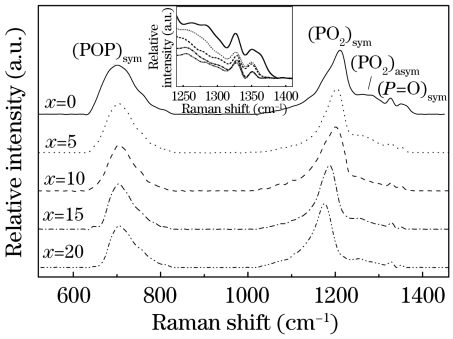

Fig. 1. Raman spectra of the phosphate glasses with x mol% SiO_2 addition ($x = 0$, 5, 10, 15, and 20).

Figure 1 indicates that the structural network of glass samples is mainly constructed by Q^2 and Q^3 units. The fraction of Q^2 and Q^3 units in sodium ultraphosphate glass (aNa$_2$O-bP$_2$O$_5$, $a < b$) can be predicted by the following formulas[10]:

$$f(Q^3) = \frac{b-a}{b}, \tag{1}$$

$$f(Q^2) = 1 - f(Q^3). \tag{2}$$

According to previous Nuclear Magnetic Resonance analysis[13], $[SiO_4]$ tetrahedrons and $[SiO_6]$ octahedrons coexist in sodium phosphate glasses containing SiO_2. And especially, it should be noted that $[SiO_4]$ unit is charge balanced while $[SiO_6]$ unit is negative charged. In phosphate glass, $[SiO_4]$ units do not change the fraction of Q^2 and Q^3 just because they are charge balanced. In our glass system, if we neglect the influence of Al_2O_3 and RE_2O_3 since their contents change unremarkably, and if we assume that SiO_2 only exists in the form of $[SiO_4]$, $f(Q^3)$ and $f(Q^2)$ can be calculated by Eqs. (1) and (2). The result is, as the SiO_2 content increases from 0 to 5 mol%, $f(Q^3)$ only decreases from 0.80 to 0.79 and $f(Q^2)$ increases from 0.20 to 0.21. This can not explain the significant decrease for the intensity of P=O mode when 5 mol% SiO_2 is added to the glass. The above assumption that all of SiO_2 only exist in the form of $[SiO_4]$ is not suitable for our glass system. The decrease in P=O stretching intensity indicates that some of Si^{4+} ions form $[SiO_6]$ octahedrons, which coordinate with the terminal oxygen in Q^3 units and turn the P=O bond into P-O-Si bond, for $[SiO_6]$ octahedrons are able to compensate the charge of pentavalent phosphorus.

Based upon the evolution of Raman spectra in the region of $1300 - 1350$ cm^{-1}, there are two stages for the coordination of SiO_2 added into our glass system. When small amount of SiO_2 is introduced into our phosphate glass, most of the Si^{4+} ions form $[SiO_6]$ and incorporate with P=O bond, thus the quantity of P=O bond decreases very fast. With further addition of SiO_2, the newly added SiO_2 mostly form $[SiO_4]$ which will not incorporate with P=O bond, so the amplitude of P=O stretching mode decreases much slower.

The structural information is important in interpreting the following spectroscopic properties. Figure 2 shows the absorption spectra of the glasses with different content of SiO_2 in the range from 300 to 1700 nm. The band around 976 nm is mainly from $Yb^{3+}(^2F_{5/2})$ in the glass, and the other bands are from Er^{3+} ions whose peak assignments are shown in Fig. 2. McCumber theory[14] and Judd-Ofelt theory[15,16] were performed to calculate the emission cross-section (σ_{emi}) of the transition of $Er^{3+}(^4I_{13/2}) \rightarrow Er^{3+}(^4I_{15/2})$ and Judd-Ofelt intensity parameters ($\Omega_{2,4,6}$) of Er^{3+}, respectively. The effective linewidth ($\Delta\lambda_{eff}$) of the $Er^{3+}(^4I_{13/2}) \rightarrow Er^{3+}(^4I_{15/2})$

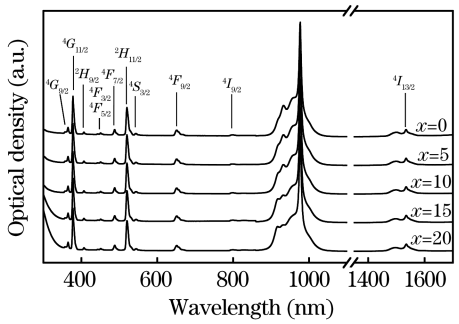

Fig. 2. Absorption spectra of the phosphate glasses with different SiO_2 addition.

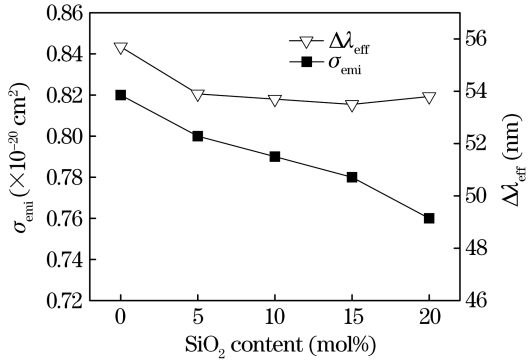

Fig. 3. Dependence of the effective linewidth and stimulated emission cross-section of $^4I_{13/2} \rightarrow {}^4I_{15/2}$ transition of Er^{3+} ions in the glasses on SiO_2 addition.

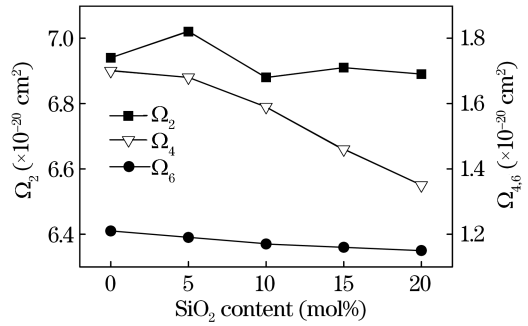

Fig. 4. Dependence of Judd-Ofelt intensity parameters (Ω_2, Ω_4, and Ω_6) of Er^{3+} ions in the glasses on SiO_2 addition.

transition is obtained from the fluorescence spectra. Figure 3 illustrates the dependences of σ_{emi} and $\Delta\lambda_{eff}$ on addition of SiO_2. Judd-Ofelt intensity parameters are plotted in Fig. 4 against SiO_2 content.

Figure 3 indicates that our Er-doped phosphate glass has comparable emission cross-section with the commercially available Er-doped glass, QX/Er (0.8×10^{-20} cm^2)[5]. With increasing introduction of SiO_2 in the glass, the emission cross-section of Er^{3+} is reduced from 0.82×10^{-20} to 0.76×10^{-20} cm^2, only decreasing by about 7%. It was reported[6] that, as the Al_2O_3 content increases from 4% to 13%, the emission cross-section of Er^{3+} decreases from 0.74×10^{-20} to 0.56×10^{-20} cm^2, decreasing by about 24%. This comparison indicates that the introduction of SiO_2 within the range of 20 mol% only brings a little influence to the spectroscopic property of Er^{3+} for our glass system. Accompanying this little change for the emission cross-section, 10.6×10^{-6} K^{-1} of the thermal expansion coefficient is decreased to 9.9×10^{-6} K^{-1}, when 10 mol% SiO_2 is added into the glass. This indicates that the thermal-mechanical property of the glass can be improved without decreasing the emission cross-section greatly.

Systematic studies[17] reveal that the value of Ω_2, one of the spectroscopic intensity parameters, increases with increasing rigidity of host matrix, and is sensitive to the local symmetry of rare-earth ions[18]. As shown in Fig. 4, Ω_2 does not show a strong dependence on SiO_2 content and has the largest value when the content of SiO_2 is 5 mol%. On the other hand, the effective linewidth of the fluorescence spectra decreases with decreasing disorder of rare-earth environment[19]. Figure 3 shows that the effective linewidth of Er^{3+} decreases from 55.7 to 53.9 nm as the SiO_2 content increases from 0 to 5 mol%, and maintains at about 53.8 nm with further addition of SiO_2. As discussed above, for the glass sample containing 5 mol% SiO_2, the introduction of SiO_2 breaks the terminal P=O bond and lengthens the bond between P^{5+} and non-bridging oxygen. Thus, Er^{3+} ions are able to be in a well ordered environment, and so the effective linewidth decreases. For the same reason, the highest value of Ω_2 at 5 mol% SiO_2 addition may be due to the formation of P–O–Si bond. The average bond length between P^{5+} and non-bridging oxygen continue to increase with further addition of SiO_2, but the number of P=O bonds decreases much slower when SiO_2 content is larger than 5 mol%. It should be noted that the effective linewidth remains nearly unchanged in the glasses containing $5-20$ mol% SiO_2, suggesting that the number of P=O bonds is the decisive factor of effective linewidth.

Ω_4 and Ω_6 of the spectroscopic intensity parameters are related to the covalency between Er^{3+} ions and O^{2-} ions, and increase with decreasing the covalency[17,20]. With introducing SiO_2 to phosphate based glass, there are silicon-oxide polyhedrons to be formed in the glass. At this time, a part of Er^{3+} ions that are only coordinated with $[PO_4]$ units, will be also affected at a distance by silicon-oxide polyhedrons. That is to say, Er^{3+} ions in our SiO_2-containing phosphate glass are surrounded by O^{2-} ions that incorporated with P^{5+} and Si^{4+}. The bonding situation of P-O and Si-O will determine the bonding covalency between Er^{3+} and O^{2-}. The covalency between Er^{3+} and silicon-oxide polyhedron is larger than that between Er^{3+} and phosphor-oxide polyhedron[21].

Figure 4 shows that Ω_4 and Ω_6 decrease with the addition of SiO_2, indicating that the covalency between Er^{3+} and O^{2-} is increased. This increase for the bonding covalency means that the interaction force between P^{5+} and O^{2-} is weakened, because the polarization of Er^{3+} by O^{2-} is strengthened[21]. Most probably, the bond between P^{5+} and O^{2-} is lengthened due to the introduction of SiO_2.

As above statement for the Raman spectra in Fig. 1, the $(PO_2)_{sym}$ mode shifts from 1210 to 1175 cm^{-1} with increasing addition of SiO_2. Since the bridging oxygen is hardly affected by Si^{4+} in the glass, the average bond length between P^{5+} and non-bridging oxygen will be most probably lengthened. It should be pointed out that such a deduction, regarding the influence of SiO_2 introduction on the glass structure, is almost the same with that deduced from the analysis of the spectroscopic in-

tensity parameters.

In conclusion, the structural characteristics and spectroscopic properties of Na_2O-Al_2O_3-P_2O_5-$x SiO_2$ glasses with $0-20$ mol% SiO_2 addition were investigated. Raman and Judd-Ofelt spectroscopic analysis reveal that the addition of SiO_2 does not dramatically change the glass structure and spectroscopic properties, and the emission cross-section of Er^{3+} decreases by only 7%. The result indicates that, by a proper addition of SiO_2, it is possible to obtain a new promising Er-doped phosphate based glass which the thermal-mechanical properties can be improved and the laser performance will be almost maintained.

This work was supported by the International Cooperation Project of Shanghai Municipal Science and Technology Commission under Grant No. 05S207103.

References

1. V. P. Gapontsev, S. M. Matitsin, A. A. Isineev, and V. B. Kravchenko, Opt. Laser Technol. **14,** 189 (1982).
2. S. Jiang, J. D. Myers, R. Wu, G. M. Bishop, D. L. Rhonehouse, M. J. Myers, and S. J. Hamlin, Proc. SPIE **2379,** 17 (1995).
3. F. Zhao, Q. Dong, and L. Hu, Chin. Opt. Lett. **5,** 41 (2007).
4. Z. Liu, C. Qi, S. Dai, Y. Jiang, and L. Hu, Chin. Opt. Lett. **1,** 37 (2003).
5. S. Jiang, M. Myers, and N. Peyghambarian, J. Non-Cryst. Solids **239,** 143 (1998).
6. Z. Liu, L. Hu, D. Zhang, S. Dai, C. Qi, and Z. Jiang, Acta Phys. Sin. (in Chinese) **51,** 2629 (2002).
7. T. Izumitani and H. Toratani, D. E. Patent 3,435,133 (1985).
8. Z. Jiang, Chinese J. Lasers (in Chinese) **33,** 1165 (2006).
9. C. Nelson and D. R. Tallant, Phys. Chem. Glasses **25,** 31 (1984).
10. J. J. Hudgens, R. K. Brow, D. R. Tallant, and S. W. Martin, J. Non-Cryst. Solids **223,** 21 (1998).
11. R. K. Brow, J. Non-Cryst. Solids **263&264,** 1 (2000).
12. A. M.-Milankovic, A. Gajovic, A. Santic, and D. E. Day, J. Non-Cryst. Solids **289,** 204 (2001).
13. R. Dupree, D. Holland, and M. G. Mortuza, Nature **328,** 416 (1987).
14. W. J. Miniscalco and R. S. Quimby, Opt. Lett. **16,** 258 (1991).
15. B. R. Judd, Phys. Rev. **127,** 750 (1962).
16. G. S. Ofelt, J. Chem. Phys. **37,** 511 (1962).
17. H. Desirena, E. De la Rosa, L. A. Diaz-Torres, and G. A. Kumar, Opt. Mater. **28,** 560 (2006).
18. H. Xia, J. Zhang, J. Wang, and Y. Zhang, Chin. Opt. Lett. **4,** 476 (2006).
19. P. M. Peters and S. N. Houde-Walter, J. Non-Cryst. Solids **239,** 162 (1998).
20. S. Tanabe, T. Ohyagi, S. Todoroki, T. Hanada, and N. Soga, J. Appl. Phys. **73,** 8451 (1993).
21. F. Gan, *Optical and Spectroscopic Properties of Glass* (Springer-Verlag Berlin Heidelberg and Shanghai Scientific and Technical Publishers, 1992) pp.148 – 203.